

# Accommodating Homeostatically Stable Dynamical Regimes to Cope with Different Environmental Conditions

Bruno A. Santos<sup>1,2</sup>, Phil Husbands<sup>1</sup> and Tom Froese<sup>1</sup>

<sup>1</sup>Centre for Computational Neuroscience and Robotics, University of Sussex, Brighton, U.K.

<sup>2</sup>Computer Engineering Department, CEFET-MG, Belo Horizonte, Brazil.  
brandre@gmail.com

## Abstract

Does the dynamical regime in which a system engages when it is coping with a situation *A* change after adaptation to a new situation *B*? Is homeostatic instability a generic mechanism for flexible switching between dynamical regimes? We develop a model to approach these questions where a simulated agent that is stable and performing phototaxis has its vision field inverted so that it becomes unstable; instability activates synaptic plasticity changing the agent's simulated nervous system attractor landscape towards a configuration that accommodates stable dynamics under normal and inverted vision. Our results show that: 1) the dynamical regime in which the agent engages under normal vision changes after adaptation to inverted vision; 2) homeostatic instability is not necessary for switching between dynamical regimes. Additionally, during the dynamical system analyses we also show that: 3) qualitatively similar behaviours (phototaxis) can be generated by different dynamics; 4) the agent's simulated nervous system operates in transient dynamic towards an attractor that continuously move on the phase space; and 5) plasticity moves and reshapes the attractor landscape in order to accommodate a stable dynamical regimes to deal with inverted vision.

## Introduction

The concept of homeostasis coined by Cannon (1932) refers to a condition in which coordinated physiological processes maintain certain variables within limits. Though this concept was introduced by Cannon, earlier work by Bernard (1927) had already identified regulatory systems in the organism's internal environment (*milieu interieur*). From these pioneering works, research in animal physiology studied homeostatic mechanisms controlling body temperature, heart rate, levels of blood sugar, breathing rate and others (see Cooper (2008) for a historical review). Recently, Turrigiano et al. (1998) observed that neurons also have a mechanism of homeostatic regulation which increases or decreases the strength of their synaptic inputs ensuring the maintenance of their firing rates within boundaries. She has also reported the presence of homeostatic regulations of activity in cortical networks (Turrigiano, 1999; Turrigiano and Nelson, 2004).

Rather than working directly with physiology, Ashby (1947, 1960) focused on more abstract dynamical system models of homeostasis in the context of adaptive behaviour. According to him, an animal behaviour is adaptive if it maintains essential variables within physiological limits. These variables are closely related to survival; they can be lethal (e.g. amount of oxygen in the blood), or only represent some approaching threat (e.g. heat on the skin). When essential variables cross certain boundaries a mechanism that changes the system configuration is activated until these variables return to homeostatic stable regions. The mechanism that pushes the variables back to their viable regions selects those configurations that not only recover stability at the current moment, but also leave the system stable in the presence of environmental conditions to which the system has previously adapted.

To illustrate the operation of this mechanism, consider an animal (*A*) interacting with its environment (*E*) (Fig. 1 represents the dynamic of *A* and *E* over time (*T*)). When the environment changes (at *t*<sub>2</sub>) the animal's dynamic becomes homeostatically unstable (the homeostatic boundary is represented by the dashed line). Due to instabilities the mechanism that changes the animal's organization is activated (downstrokes at *M*). The new organization found by *M* leaves the animal stable in the presence of both environmental conditions, as it is shown by the animal's dynamic (*A*) at *t*<sub>4</sub> and *t*<sub>5</sub>.

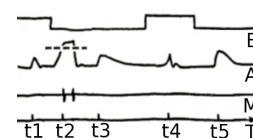


Figure 1: See text.  
Adapted: Ashby (1960) p.116.

Ashby also postulated that different environmental conditions can move the state of the system to different regions in phase space and at each region the system can have different dynamics. This is roughly illustrated by different dynamical regimes presented by the animal at *t*<sub>4</sub> and *t*<sub>5</sub>. Summing up Ashby's main points in the context of our work, we can say that: an adaptive system interacting with its environment switches and engages in different dynamical regimes; when homeostatic instability increases the system reconfigures itself so that it: 1) accommodates a stable dynamical regime

that deals with the condition that triggered instability; and 2) maintains the stability of pre-existing dynamical regimes that deal with conditions previously adapted.

The homeostatic characteristics of a system do not impose constraints on the dynamics inside stable regions. As long as the state of the system is inside a homeostatic region, the system can be in an attractor or moving on a transient; it can also be monostable, bistable, multistable, or even without attractors inside stable regions. Thus, at the same time two types of stability can be measured in a system: homeostatic stability and Lyapunov stability<sup>1</sup>.

Both stabilities are illustrated in Fig. 2. The axes  $X_1$  and  $X_2$  represent two generic variables; the dashed line is the homeostatic stable region;  $P_1$  and  $P_2$  are point attractors; continuous line around  $P_1$  and  $P_2$  define two regions on the phase space. On the border between these regions the system is Lyapunov unstable; outside the dashed line the system is homeostatically unstable. The point  $P_3$  is homeostatically stable and Lyapunov unstable. Both types of stability are important to studying mechanisms of behavioural adaptation, but in this paper we focus exclusively on homeostatic stability.

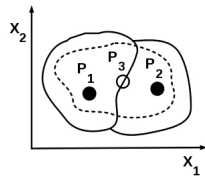


Figure 2: See text.

Given this brief introduction about homeostatic stability and adaptation, we present the questions we are tackling in this paper.

- Q1: Does the dynamical regime in which the system engages when it is coping with a situation  $A$  change after adaptation to a new situation  $B$ ?

Using the illustration presented in Fig. 1 we can restate this question as: does the dynamical regime in which the animal engages when it is coping with the environmental condition presented at  $t_1$  change after adaptation to the new environmental condition presented at  $t_2$ ? We want to know the difference between the dynamics at  $t_1$  and  $t_4$ , as the system has reorganized itself in order to accommodate a new stable dynamical regime to cope with the environmental condition presented at  $t_2$ .

While the previous questions concerns the mechanism for adaptation, the second one approaches the mechanism for switching between dynamical regimes after adaptation.

- Q2: After adaptation, is homeostatic instability a generic mechanism for flexible switching between dynamical regimes?

Using the illustration presented in Fig. 1 we can restate this question as: is homeostatic instability a generic mech-

<sup>1</sup>A fixed point  $x^*$  is Lyapunov stable if all trajectories that start sufficiently close to  $x^*$  remain close to it for all time. For a formal definition of Lyapunov stability see Strogatz (2000) p.141.

anism for flexible switching between dynamical regimes in which the animal engages at  $t_4$  and  $t_5$ ?

In order to approach these questions we develop a computational model based on a related model implemented by Di Paolo (2000). In his model, Di Paolo minimally replicated a psychological experiment carried out by Taylor (1962) where a human being adapts his behaviour to continuously wearing spectacles that distorts his vision field. Di Paolo replicated this experiment using an evolved simulated agent that performs phototaxis. During the agent's lifetime, he inverted the agent's vision field (switching right and left sensors) and studied the process of behavioural adaptation. The agent's mechanism of adaptation was implemented using homeostatic stability and synaptic plasticity<sup>2</sup>.

Following Di Paolo we implement an agent performing phototaxis using homeostatic stability and synaptic plasticity. However, we replicate another experiment carried out by Taylor where a subject adapts his behaviour to intermittently (rather than continuously) wearing spectacles that distorts his vision field. Besides, in our model the inversion of the agent's vision field is done both during its lifetime and during evolution. Thus, our agent is evolved to adapt during its lifetime to inverted vision, differing from Di Paolo's agent which was evolved exclusively to perform phototaxis under normal vision.

The methodology to develop our computational model is based on four assumptions. The first three assumptions are grounded in Ashby's theory in the context of Turriano's empirical findings on homeostasis in neuronal networks, they are: 1) an agent behaviour is adaptive if it maintains its simulated neuronal network homeostatically stable; 2) changes in synapse strengths is a mechanism to recover homeostatic stability; and 3) a system conserves its condition of being adapted when synapse strengths are adjusted in such a way that homeostatic stability of neuronal networks is maintained in the presence of similar conditions that triggered instability in the past. The fourth assumption, which is supported by Ashby and Taylor<sup>3</sup>, is that: 4) conditions to which the system is not adapted trigger homeostatic instability, that is, switching visual sensors triggers homeostatic instability in a not-yet-adapted simulated nervous system.

Details of the methodology are presented on the next section, followed by the Results where we study the dynamic of the system and show that: 1) the dynamical regime in which the agent engages under normal vision changes after adaptation to inverted vision; 2) homeostatic instability is not necessary for switching between dynamical regimes. Additionally, during the dynamical system analyses we also show that: 3) qualitatively similar behaviours (phototaxis)

<sup>2</sup>For a theoretical discussion of Di Paolo's model see Di Paolo (2003).

<sup>3</sup>Taylor, in his experiment, uses Ashby's theory to explain the operation of the mechanism underlying the adaptive behaviour presented by the subject wearing distorted spectacles.

can be generated by different dynamics; 4) the agent's simulated nervous system operates in transient dynamic towards an attractor that continuously moves in the phase space; 5) plasticity moves and reshapes the attractor landscape in order to accommodate a stable dynamical regimes to deal with inverted vision.

## Methods

This methodology follows, as much as possible, that one carried out by (Di Paolo, 2000). The main differences lie in the number of nodes used to implement the controller and in the evolutionary setup.

A genetic algorithm is used to evolve the parameters of our model. The range of each parameter, which defines the search space, is presented throughout the methodology together with the description of each variable.

**Task.** The task involves an agent that moves in a simulated environment and has to perform phototaxis on a sequence of light presentations (one by one) for 15000 secs. During its lifetime, the agent's right and left sensors are switched every 250 secs. The light is repositioned between 40 and 80 units away from the agent when either the sensors are switched or the agent spends 50 consecutive seconds close light (at a distance smaller than 10 unit).

**Agent.** The agent (Fig. 3) has a circular body of 8 units diameter, two diametrically opposed motors that receive a continuous signal in the range  $[-1,1]$  from the controller nodes ( $y_2$  and  $y_3$ , respectively), and two light sensors separated by  $120^\circ \pm 10^\circ$  whose output signal is given by  $I_k = 1/\sqrt{d_k}$ , where  $k$  represents each sensor,  $d$  is the distance from sensor  $k$  to the light source.  $I_k = 0$  when the agent's body occludes the light and  $I_k = 1$  if  $d < 1$ .

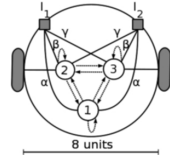


Figure 3: Agent.

**Plastic controller.** The agent's behaviour is controlled by a fully-connected, 3 nodes, continuous-time recurrent neural network (Eq. 1) (Beer, 1995).

$$\begin{aligned} \tau_i \dot{y}_i &= -y_i + \sum_{j=1}^N w_{ji} z_j + \sum_{k=1}^M s_{ki} I_k, \\ z_i &= \frac{1}{1 + e^{-(y_i + b_i)}} \end{aligned} \quad (1)$$

where  $y$  is the state of each node which is integrated with time step of 0.1 using the Euler method,  $\tau$  is its time constant (range  $[0.4,4]$ ,  $N$  is the number of CTRNN nodes (here 3);  $w_{j,i}$  is the connection strength from the  $j^{th}$  to  $i^{th}$  node (range  $[-8,8]$ ),  $z_j$  is the node output signal defined by a sigmoid function,  $b_j$  is a bias (range  $[-3,3]$ ),  $M$  is the number of inputs (here 2);  $I_k$  is the sensory output signal, and  $s_{ki}$  is a constant that represents the sensory strength from the  $k^{th}$  sensor to  $i^{th}$  node. The values for  $s_{ki}$  are:

$s_{11} = s_{21} = \alpha$ ;  $s_{12} = s_{23} = \beta$ ;  $s_{13} = s_{22} = \gamma$ , where  $\alpha$ ,  $\beta$  and  $\gamma$  are in the range  $[0.01,10]$  (see Fig. 3). Each connection between nodes ( $w_{j,i}$ ) is adjusted by one out of four different homeostatic plastic rules (2). The rule used by each connection is defined by the genetic algorithm.

$$\begin{aligned} R0 : \Delta w_{ji} &= \delta \eta_{ji} p_i z_j z_i, \\ R1 : \Delta w_{ji} &= \delta \eta_{ji} p_i (z_j - z_{ji}^o) z_i, \\ R2 : \Delta w_{ji} &= \delta \eta_{ji} p_i (z_i - z_{ji}^o) z_j, \\ R3 : \Delta w_{ji} &= 0, \end{aligned} \quad (2)$$

where  $\Delta w_{ji}$  is the change in  $w_{ji}$ ,  $\delta$  is a linear damping function that constrains the weights between allowed values  $[-8,8]$ ,  $\eta_{ji}$  is the rate of change (range  $[-0.9,0.9]$ , and  $p_i$  is the plastic facilitation defined by the function shown in the Fig. 4. Rule 0 is the Hebbian and anti-Hebbian rules (depending on  $p_i$  and  $n_{ji}$ ); rules 1 and 2 potentiate or depress the connection depending on how presynaptic or postsynaptic node activity relates to a threshold  $z_{ji}^o$ . This threshold linearly depends on  $w_{ji}$  ( $z_{ji}^o = 0$  if  $w_{ji} = -8$  and  $z_{ji}^o = 1$  if  $w_{ji} = 8$ ).

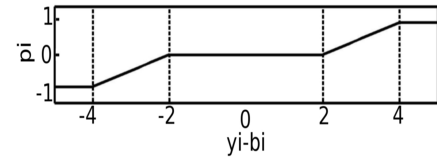


Figure 4: Local plasticity facilitation  $p_i$ . When the node activation minus its bias ( $y_i - b_i$ ) is in the stable region  $[-2, 2]$  plasticity is not activated as  $p_i = 0$ . Out of this region  $p_i$  changes either positively or negatively according to the function.

**Evolutionary setup.** A total of 36 network parameters encoded in a genotype as a vector of real numbers in the range  $[0,1]$  are evolved using the microbial genetic algorithm (Harvey, 2001) and linearly scaled, at each trial, to their corresponding range. The genetic algorithm is setup as follows: population size (100); mutation rate (0.05); recombination (0.60); reflexive mutation; normal distribution for mutation ( $\mu = 0, \sigma^2 = 0.1$ ); and trials for each agent (8). At the end of the 8<sup>th</sup> trial the worst fitness (out of 8) is used as the fitness of the agent.

The agent's lifetime is 15000 seconds and its sensors are inverted every 250 seconds. In total, sensors are inverted 60 times, where 30 times the agent is under normal vision and 30 under inverted vision. At each timeslot (250 secs) the fitness of the agent is measured according to Eq. 3:

$$F_t = \frac{F_b + F_s}{2} \quad (3)$$

where  $t$  is the timeslot (out of 60),  $F_b$  is the behavioural-fitness (Eq. 4) and  $F_s$  is the stability-fitness (Eq. 3).

$$F_b = \left( P + \left( 1 - \frac{d_f}{d_i} \right) \right) \frac{R}{T} \quad (4)$$

where  $d_i$  and  $d_f$  are initial and final distances to the light source, respectively, and  $d_f$  is clipped at 0 when  $d_f > d_i$ ;  $P$  is the number of times the agent approaches the light in the current timeslot (the agent can approach the light more than once as the light moves when the agent spends 50 seconds near it);  $T$  is the timeslot length (250 secs) and  $R$  (250 secs) is the required time given to the agent to approach a light source. During evolution, as  $T=R$  the agent should approach the light at least once in order to obtain  $F_b = 1$ . When the agent approaches the light more than the number of times required,  $F_b$  is clipped at 1.

$$F_s = \frac{1}{1 + e^{\left(\frac{u}{70} - 7\right)}} \quad (5)$$

where  $u$  is the number of times the nodes activate out of the stable region (at each Euler step, it can be incremented by 3 when the three nodes activate out of the stable region); the constants 70 and 7 define the shape of the function.

The total fitness of the agent is given by the weighted mean of the fitness at each timeslot.

$$F = \frac{1}{3K} \sum_{t=1}^K q_t; \quad q_t = \begin{cases} F_t; & \text{if } v = 1 \wedge \forall t \\ 2(1 - F_t); & \text{if } v = -1 \wedge t \leq 30 \\ 2F_t; & \text{if } v = -1 \wedge t > 30 \end{cases} \quad (6)$$

where  $K$  is the number of timeslots (out of 60);  $F_t$  is defined in Eq. 3;  $v$  is the vision state (1 normal, -1 inverted). Under normal vision ( $v=1$ ) the agent should get high fitness ( $F_t$ ) during its whole lifetime ( $\forall t$ ). Under inverted vision the agent should have low fitness ( $F_t$ ) during the first 30 inversions ( $t \leq 30$ ) and high fitness during the last 30. Hence: 1) the agent should perform phototaxis maintaining homeostatic stability under normal vision during the whole trial (30 timeslots); 2) the agent should be homeostatically unstable and not perform phototaxis when its vision field is inverted; and 3) over time, after a sequence of vision inversions (normal  $\rightarrow$  inverted  $\rightarrow$  normal  $\rightarrow$  inverted, and so on), the agent should maintain stability and perform phototaxis under inverted vision (the last 30 timeslots).

After evolution the best agent of the population was selected and run 10000 in order to generate statistical measurements. The agent's lifetime was changed to 30000 secs and after 15000 secs of its lifetime its sensors were switched at a different frequency (as shown in Fig. 5-D).

**Attractor landscape.** In order to find the attractors of the controller while the agent is interacting with its environment, a snapshot of the system is taken at

each Euler step of the agent's lifetime and the limit  $\lim_{t \rightarrow \infty} \langle y_1(t), y_2(t), y_3(t) \rangle$  is numerically estimated. This snapshot consists of states of each CTRNN node ( $y_1, y_2, y_3$ ), which are the initial conditions to find the limit; connection weights ( $w_{ji}$ ); inputs ( $I_1$  and  $I_2$ ), which are maintained fixed during the numerical estimation; sensor strengths ( $s_{ki}$ ), biases ( $b_i$ ); and time constants ( $\tau_i$ ).

The limit is found using Euler integration with time step 0.1 and 900000 steps. When the system does not converge to a point attractor, the Euler integration runs for a further 100000 steps in order to capture at least some points of either the limit cycle or the strange attractor the system is assumed to be following.

## Results

**Evolution.** The mean fitness of the population after evolution is 0.77 and the fitness of the best agent is 0.86. In Fig. 5-A and B (see caption) we present how the behavioural-fitness and stability-fitness of the best agent change during its lifetime.

Under normal vision the behavioural-fitness and the stability-fitness are maintained near 1 over the whole simulation. At the beginning of the agent's lifetime and under normal vision, the number of unstable activations is near 200. Despite these unstable activations the stability-fitness is still high due to the shape of the function defined in (5). Under inverted vision, the behavioural-fitness starts near 0 and linearly increases during the first 10000 secs; while the stability-fitness increases mainly between 5000 secs. and 10000 secs. These fitnesses increase at a different rate because while the activations of the nodes move towards the stable region, the behavioural-fitness increases; on the other hand, the stability-fitness only increases when the activations actually cross the boundaries (range [-2,2]), which starts after 5000 secs.

**Behaviour.** The distances from the agent to the light source before and after adaptation are presented in Fig. 6-A and B, respectively. After the first inversion (Fig. 6-A,  $t = 251$  secs) the agent keeps turning around itself and only slightly moves towards the light until its sensors are switched back to the normal position ( $t=500$  secs). After adaptation the agent approaches the light under both conditions.

**Dynamics.** The dynamical patterns in which the agent engages are represented in 6 dimensions (S1, S2: sensors; M1-M2: motors;  $y_1, y_2, y_3$ : CTRNN nodes) by each pair of graphs in Fig 7 (see figure caption). From now on the dynamics of the CTRNN nodes presented in Fig 7-A, B, C and D will be referred as  $\rho_1, \rho_2, \rho_3$  and  $\rho_4$ , respectively.

At the beginning of its lifetime, the agent engages in a homeostatic stable dynamical pattern ( $\rho_1$ ) while performing phototaxis. Just after the first inversion the agent switches

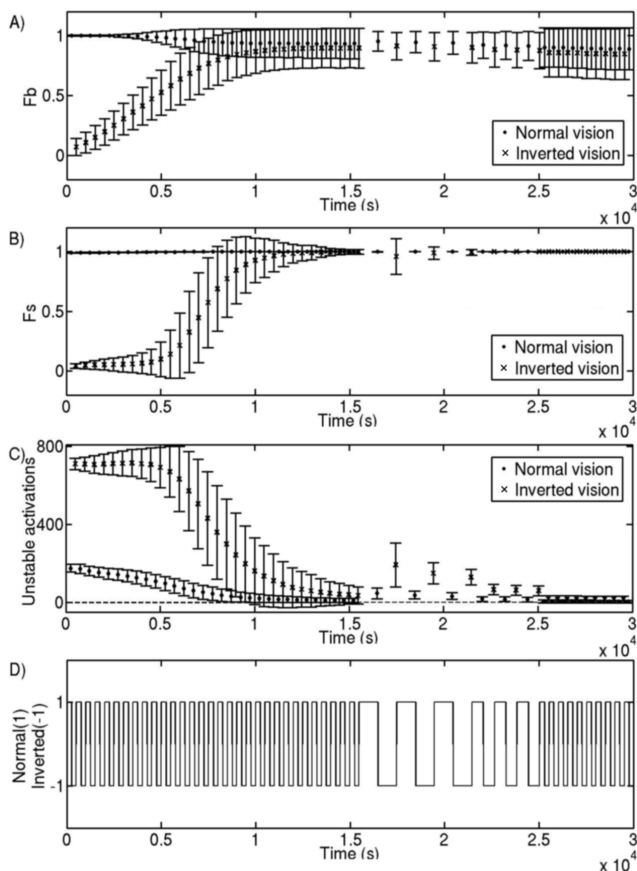


Figure 5: **A** and **B** show how behavioural-fitness and stability-fitness change over the agent’s lifetime. Each point in those graphics represents the fitness for a specific timeslot. **C** depicts the number of node activations out of the stable region. **D** depicts the frequency of sensor switchings. These plots were generated running the best agent over 10000 trials. The vertical bars represent the standard deviation.

to the unstable  $\rho_2$ . After a sequence of inversions and plastic changes, the dynamical pattern instability under inverted vision decreases and changes from the unstable  $\rho_2$  to the stable  $\rho_4$ . While instability under inverted vision decreases, the stability under normal vision is maintained (as shown in Fig 5-B); however, even while maintaining stability the dynamics under normal vision qualitatively changes from  $\rho_1$  to  $\rho_3$  as a side effect of adaptation to inverted vision.

While plasticity is activated during adaptation to inverted vision (from  $t=250$  to  $t=15000(s)$ ), the dynamical patterns under normal vision smoothly change from  $\rho_1$  to  $\rho_3$ . In between these patterns there are other slightly different dynamical patterns and all of them generate phototactic behaviour (as shown by the behavioural-fitness - Fig 5-A). Besides the dynamical patterns under normal vision,  $\rho_4$  under inverted vision also generates phototaxis. This shows that qualita-

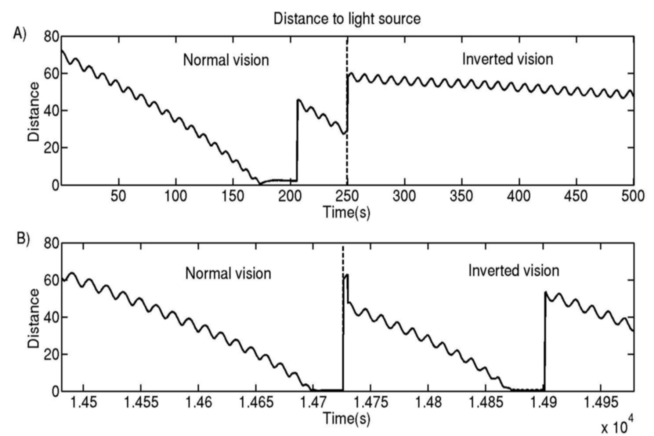


Figure 6: Distance from the agent to the light source before and after adaptation (**A** and **B** , respectively).

tively the same behaviour can be generated by different dynamics.

The dynamical patterns in which the agent engages are generated by an attractor that continuously moves in the phase space. This continuous movement of the attractor leaves the agent in a transient state while interacting with its environment (see Fig. 8). The transient dynamic is obtained because different sensor values define different set of parameters for the CTRNN equations which in turn gives different point attractors at each iteration. In other words, the agent’s behaviour (movement in the environment) changes its sensor values which in turn moves the attractor in the phase space. The direction to which the attractor pulls the system generates new motor outputs that change the agent’s position and consequently its sensor values. The resulting dynamical patterns involving the controller, body and environment generate the coordinated movement of the agent towards the light source.

While sensors values are changing and the rate of plastic changes is low, that is, when the agent is engaged in a stable dynamical pattern while interacting with its environment, the point attractor moves on a fixed 3D surface. At the beginning of the agent’s lifetime this surface resembles a rectangle with attractors lying on its corners (see Fig.9 - gray dots). After adaptation, this surface moves to a different position and is reshaped (see Fig.9 - black dots). This new position and shape of the attractor landscape accommodates the stable dynamical patterns under normal and inverted vision, that is, both dynamical patterns  $\rho_3$  and  $\rho_4$  are generated by the same attractor landscape.

A quantitative difference between surfaces of attractors for each dynamical pattern ( $\rho_1$ ,  $\rho_2$ ,  $\rho_3$  and  $\rho_4$ ) is shown by the positions of clusters of attractors<sup>4</sup> (see Fig. 10-A1, B1,

<sup>4</sup>We used the K-means method (MacQueen, 1967) to identify clusters of attractors and their centroids.

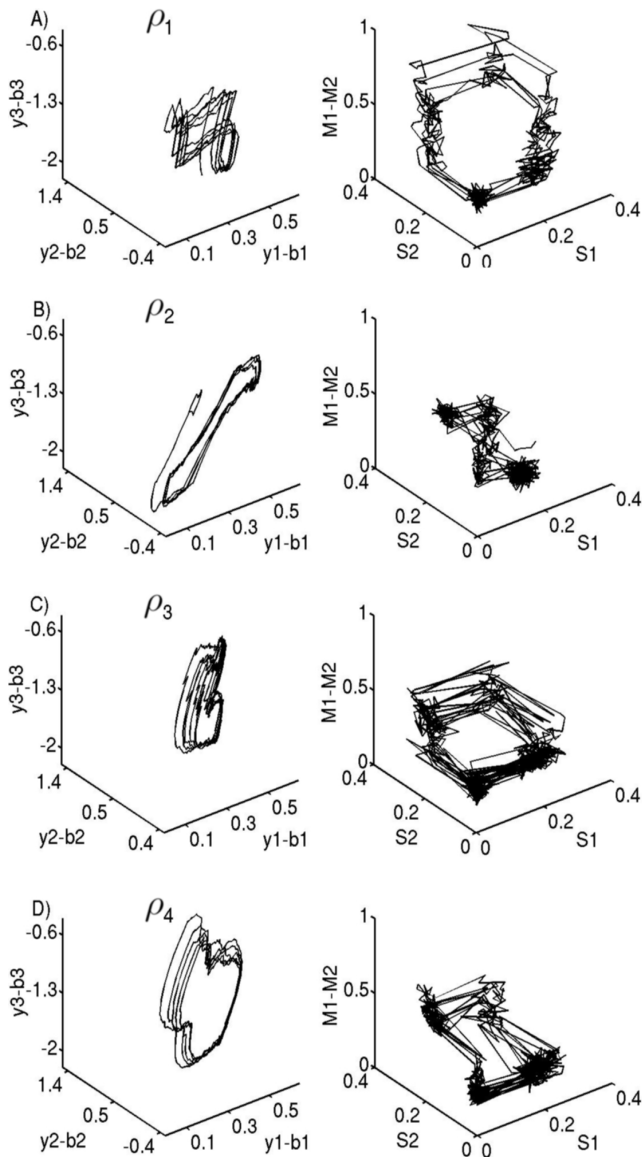


Figure 7: **A)** Stable dynamical pattern under normal vision before the first inversion; time: 85.7 to 137.0 secs; initial distance  $d_i = 40.17$ ; final distance  $d_f = 20.2$ . **B)** Unstable dynamical pattern during the first inversion; time: 250.2 to 300.0 secs;  $d_i = 57.75$ ;  $d_f = 57.84$ . **C)** Stable dynamical pattern under normal vision after adaptation; time: 14569.9 to 14650.2 secs;  $d_i = 40.06$ ;  $d_f = 20.09$ . **D)** Stable dynamical patterns under inverted vision after adaptation; time: 14749.7 to 14818.5 secs;  $d_i = 40.02$ ;  $d_f = 20.01$ .

C1, and D1). Comparing the centroid positions for  $\rho_1$  and  $\rho_3$  we see how the surface changed for normal vision after adaptation to inverted vision. Comparing the centroid positions for  $\rho_3$  and  $\rho_4$  we see that the surfaces after adaptation are qualitatively the same under normal and inverted vision. The new shape and position of the attractor surface

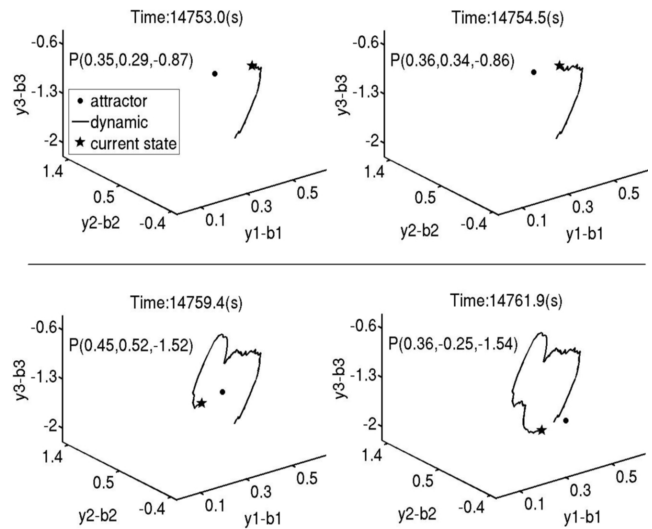


Figure 8: Four snapshots depicting the agent's transient internal dynamic while engaged in  $\rho_4$ . (time interval: [14753.0, 14761.9] secs.).  $P(y_1-b_1, y_2-b_2, y_3-b_3)$  indicates the attractor position.

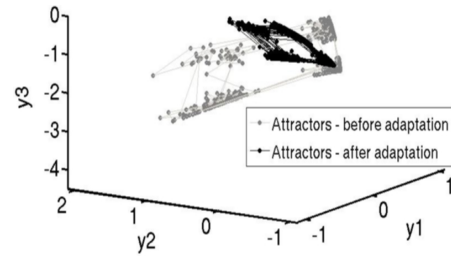


Figure 9: Surfaces defined by the movement of point attractors when the agent is doing phototaxis under normal vision before (gray) and after adaptation (black). Time intervals [85.7,137.0] and [14569.9, 14650.2] secs, respectively.

after adaptation is caused by plastic changes that are activated when the system is homeostatic unstable.

Though the attractor surfaces are qualitatively the same after adaptation, the way the attractors move on the surface is different under normal and inverted vision. That is the reason why  $\rho_3$  and  $\rho_4$  are different (see Fig. 10-A2, B2, C2, and D2). While  $\rho_3$  is generated by the movement of an attractor between the four clusters in the order  $4 \rightarrow 3 \rightarrow 2 \rightarrow 1$ ,  $\rho_4$  is generated by  $1 \rightarrow 2 \rightarrow 3 \rightarrow 4$ .

Switching between dynamical regimes (e.g. switching from  $\rho_3$  to  $\rho_4$ ) does not require homeostatic instability. At the end of the agent's lifetime, after many plastic activations, the agent switches between the dynamical patterns without activation out of its viable region (see Fig. 11).

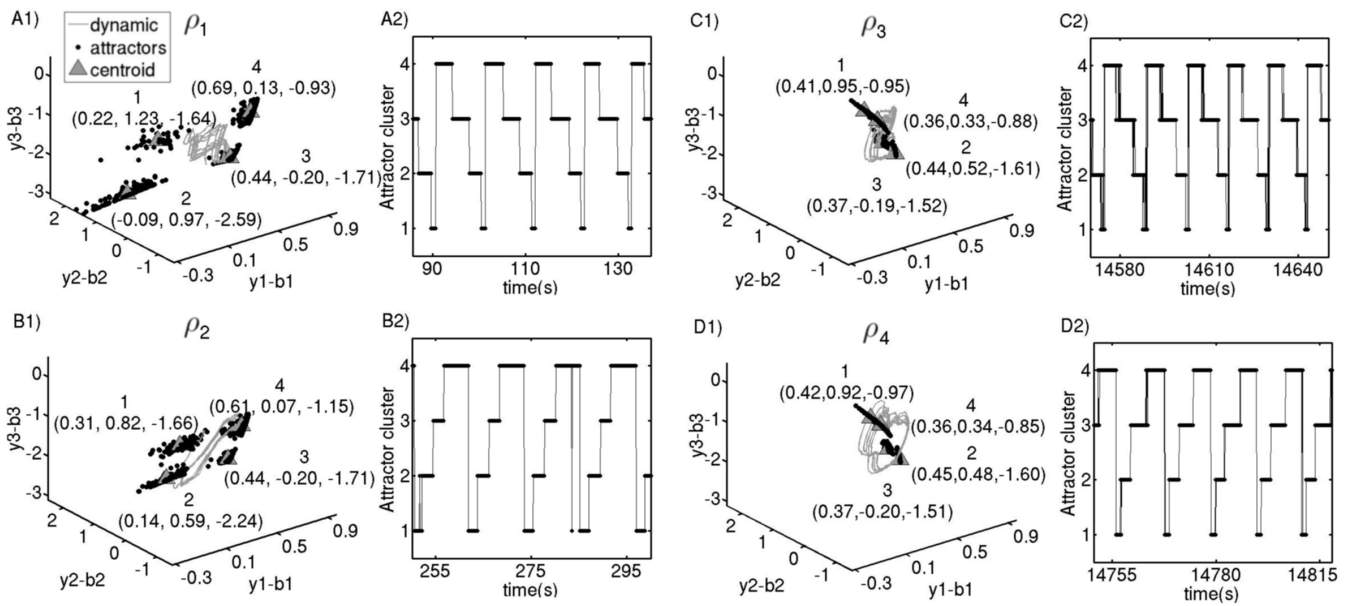


Figure 10: Phase space (*A1*, *B1*, *C1* and *D1*) depictions: dynamics of the internal nodes (gray lines); point attractors and attractor layout (black dots); cluster centroids (numbering from 1 to 4). Temporal sequence of the movement of attractors (*A2*, *B2*, *C2* and *D2*) shows how the attractors move between clusters over time. The time intervals to generate these graphs are the same as those in Fig 7

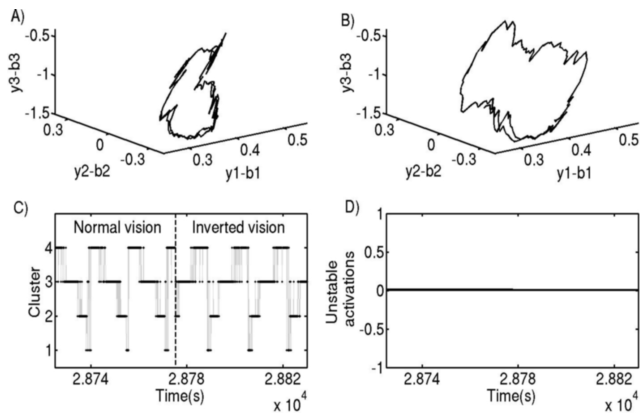


Figure 11: **A** and **B** depict dynamical patterns under normal and inverted vision, respectively. **C** depicts the difference between dynamic of attractors before and after inversion. **D** depicts the number of activations out of the homeostatic stable region.

## Discussion

We would like to point out some of the important implications of this model. First, it has practical importance for the design of artificial neural network systems that can learn different behaviours. It is commonly believed that when a network system learns a new behaviour, the activation of neu-

ral plasticity will perturb the existing weight configuration of previously acquired behaviours and therefore will have a detrimental effect on the systems overall performance. One traditional way to address this so-called problem of neural interference is by taking inspiration from the modular computer architecture, namely by dividing the neural system into non-overlapping neuronal groups. However, here we have demonstrated that this kind of structural modularity is not the only way for one system to realize different styles of behaviour. Even a completely integrated system can achieve behavioural differentiation because the behaviours can be generated by different dynamical regimes on the phase space.

Accordingly, the current model also has important implications for our scientific understanding of the nervous system. It is a widely held belief in neuroscience that different cognitive functions map onto distinct regions of the brain, a belief reinforced by the advent of various brain imaging methods. This appeal to structural localizability may be valid to some extent. However, the model presented in this paper is a proof of concept that this is not the only way of realizing functional differentiation. Rather than focusing on anatomical divisions alone, it is also possible to take the nervous system as one integrated system which can realize a multiplicity of behaviours by transiting between different dynamical regimes.

## Conclusion

We minimally replicated the psychological experiment described by Taylor based on assumptions drawn from Ashby's and Turrigiano's works. While Taylor's experiment shaped the desired behaviour, our assumptions constrained the dynamics of the mechanism underlying behaviour. Thus, the methodology to obtain the model we wanted to investigate incorporated restrictions on the task and on the agent's internal dynamic. Once the model was obtained we studied its dynamic in order to suggest answers to the questions Q1 and Q2 (detailed in the introduction).

In order to answer the question Q1, we showed that the dynamical regime in which the system engages under normal vision changes after adaptation to inverted vision ( $\rho_1$  changed to  $\rho_3$ ). As the system is relatively simple (only 3 CTRNN nodes) and fully-connected, even small reorganizations to accommodate new stable regimes are expected to affect pre-existing dynamics. Hence we can not generalize and say that pre-existing stable regimes always change when the system adapts to a new condition. More complex system, such as the brain, probably engages in independent dynamical regimes under different environmental conditions.

In order to answer the question Q2, we showed that homeostatic instability is not necessary for switching between dynamical regimes. This result contributes to research on brain dynamics as it complements the theoretical claim that Lyapunov instability is one generic mechanism for flexible switching among multiple attractive states; that is, for entering and exiting patterns of behaviour (Kelso, 1995). Indeed Ashby has already demonstrated that a system can switch between dynamical regimes without homeostatic instability. The difference is that, while Ashby uses the homeostat we use a more complex model where the homeostatic mechanism is intertwined with the mechanism that coordinates the movement of an agent that is continuously interacting with its environment. Thus, our investigation confirms Ashby's demonstration in a more complex environment and also complements Kelso's hypothesis about the importance of Lyapunov instability as a mechanism for switching dynamics.

We have also shown that qualitatively similar behaviours (phototaxis) can be generated by different dynamics; the agent's simulated nervous system operates in transient dynamics towards an attractor that continuously moves in the phase space; and plasticity moves and reshapes the attractor landscape in order to accommodate a stable dynamical regimes to deal with inverted vision.

## Acknowledgements

Bruno A. Santos acknowledges financial support from Brazilian National Council of Research, CNPq. Thanks to Jose Fernandez-Leon, Lucas Wilkins, Matthew Egbert, Renan C. Moiola and Xabier Barandiaran for valuable discussions, and to the reviewers of an earlier version.

## References

- Ashby, W. R. (1947). The nervous system as physical machine: With special reference to the origin of adaptive behavior. *Mind, New Series*, 56(221):44–59.
- Ashby, W. R. (1960). *Design for a brain : the origin of adaptive behaviour*. Chapman: London, 2nd edition.
- Beer, R. D. (1995). On the dynamics of small continuous-time recurrent neural networks. *Adaptive Behavior*, 3:469–509.
- Bernard, C. (1927). *An introduction to the study of experimental medicine*. Macmillan, New York.
- Cannon, W. B. (1932). *The wisdom of the body*. New York, NY, US: W W Norton & Co.
- Cooper, S. J. (2008). From claudes bernard to walter cannon. emergence of the concept of homeostasis. *Appetite*, 51:419–427.
- Di Paolo, E. A. (2000). Homeostatic adaptation to inversion of the visual field and other sensorimotor disruptions. In J. A. Meyer, A. Berthoz, D. F. H. R. and Wilson, S. W., editors, *From Animals to Animals, Proc. of the Sixth International Conference on the Simulation of Adaptive Behavior, SAB'2000*, pages 440–449. MIT Press.
- Di Paolo, E. A. (2003). *Dynamical Systems Approach to Embodiment and Sociality*, chapter Organismically-inspired robotics: homeostatic adaptation and natural teleology beyond the closed sensorimotor loop, pages 19–42. Advanced Knowledge International, Adelaide, Australia.
- Harvey, I. (2001). Artificial evolution: A continuing saga. In Gomi, T., editor, *Evolutionary Robotics: From Intelligent Robots to Artificial Life - Proc. of 8th Intl. Symposium on Evolutionary Robotics*. Springer-Verlag Lecture Notes in Computer Science LNCS 2217.
- Kelso, J. A. S. (1995). *Dynamic patterns: the self-organization of brain and behavior*. MIT Press.
- MacQueen, J. B. (1967). Some methods for classification and analysis of multivariate observations. In *Proceedings of the Fifth Symposium on Math, Statistics and Probability*, pages 281–297. Berkeley, CA: University of California Press.
- Strogatz, S. H. (2000). *Nonlinear Dynamics and Chaos: With Applications to Physics, Biology, Chemistry and Engineering*. Perseus Books.
- Taylor, J. G. (1962). *The Behavioral Basis of Perception*. New Haven: Yale University Press.
- Turrigiano, G. G. (1999). Homeostatic plasticity in neuronal networks: the more things change, the more they stay the same. *Trends in Neurosciences*, 22(5):221–227.
- Turrigiano, G. G., Leslie, K. R., Desai, N. S., Rutherford, L. C., and Nelson, S. B. (1998). Activity-dependent scaling of quantal amplitude in neocortical neurons. *Nature*, 391:892–896.
- Turrigiano, G. G. and Nelson, S. B. (2004). Homeostatic plasticity in the developing nervous system. *Nature Reviews Neuroscience*, 5:97–107.